Systematic Analysis of the Functional Overlap among Plant YTHDF proteins

Daniel Flores-Téllez, Mathias Tankmar, Junyu Chen, Peter Brodersen* and Laura Arribas-Hernández*

University of Copenhagen, Copenhagen Plant Science Center, Ole Maaløes Vej 5, DK-2200 Copenhagen N

*Corresponding authors

Email pbrodersen@bio.ku.dk (P.B.) and laura.arribas@bio.ku.dk (L.A.-H.)

Abstract

YT521-B homology (YTH) domain proteins act as readers of *N6*-methyladenosine (m^6A), the most common internal covalent modification in eukaryotic mRNA. Members of the YTHDF subclade can determine properties of m^6A-containing mRNAs in the cytoplasm of animal and plant cells. Vertebrates encode three YTHDF proteins, and whether they perform specialized or redundant molecular functions is currently debated. In land plants, the YTHDF clade has expanded from just one member in basal lineages to eleven so-called EVOLUTIONARILY CONSERVED C-TERMINAL REGION1-11 (ECT1-11) proteins in *Arabidopsis thaliana*, named after the conserved YTH domain found at the C-terminus following a long intrinsically disordered region (IDR) at the N-terminus. The origin and implications of YTHDF expansion in higher plants are not known, as it is unclear whether it involves acquisition of fundamentally different properties, in particular of their divergent IDRs. Here, we used the leaf formation defects in *ect2/ect3/ect4* mutants to test whether the many Arabidopsis YTHDF proteins can perform the same function if expressed at similar levels in leaf primordia. We show that the ancestral molecular function of the m^6A-YTHDF axis in land plants is conserved over YTHDF diversification, and currently present in all major clades of YTHDF proteins in flowering plants. Nevertheless, lineage-specific neo-functionalization of a few members also happened after late duplication events. ECT1, the closest homolog of ECT2/3/4, is one such divergent YTHDF protein. Accordingly, mutation of *ECT1* does not aggravate the defective organogenesis of *ect2/ect3/ect4* mutants, even though the four proteins are naturally expressed in the same population of primordial cells.

Significance statement

Regulation of gene expression is essential to life. It ensures correct balancing of cellular activities and the controlled proliferation and differentiation necessary for the development of multicellular organisms. Among other mechanisms, gene expression can be controlled by methylation of adenosines in mRNA (m^6A). Absence of m^6A impairs embryo development in plants and vertebrates, and its mis-regulation is associated with human cancers. m^6A-dependent regulation can be exerted by a group of cytoplasmic proteins called YTHDFs. Plants have many more YTHDFs than animals, but the reason for this is unknown. This study addresses the origin of plant YTHDF expansion, and reveals that most, but not all, have the same molecular functions that facilitate rapid division of differentiating stem cells.

Introduction

N6-methyladenosine (m^6A) is the most abundant modified nucleotide occurring internally in eukaryotic mRNA. It is of major importance in gene regulation as illustrated by the embryonic lethality of mutants in the dedicated mRNA adenosine methyltransferase in higher plants (Zhong et al., 2008) and in mammals (Geula et al., 2015). The presence of m^6A in an mRNA may have multiple biochemical consequences. These include the weakening of secondary structure (Liu et al., 2015) and the creation of binding sites for RNA-binding proteins specialized for m^6A recognition (Patil et al., 2018). YT521-B homology (YTH) domain proteins constitute the best studied class of m^6A-binding proteins. They achieve specificity for m^6A via an aromatic pocket accommodating the *N6*-adenosine methyl group, such that the affinity of isolated YTH domains for m^6A-containing RNA is 10-20-fold higher than for unmodified RNA (Li et al., 2014b; Luo and Tong, 2014; Theler et al., 2014; Wang et al., 2014a; Xu et al., 2014; Zhu et al., 2014).

Two different phylogenetic clades of YTH domains have been defined, YTHDC and YTHDF (Patil *et al.*, 2018). Genetic studies establish that major functions of m^6A in development in both vertebrates and plants depend on the YTHDF clade of readers (Arribas-Hernández et al., 2018; Arribas-Hernández et al., 2020; Murakami and Jaffrey, 2022). In all cases studied in detail thus far, YTHDF proteins are cytoplasmic in unchallenged conditions (Arribas-Hernández et al., 2021b; Balacco and Soller, 2019), and contain a long N-terminal intrinsically disordered region (IDR) in addition to the C-terminal YTH domain. While the YTH domain is necessary for specific binding to m^6A in mRNA (Patil *et al.*, 2018), the IDR is considered to be the effector part of the protein (Boo et al., 2022; Du et al., 2016; Park et al., 2019; Wang *et al.*, 2014a). Nonetheless, it has been proposed that the IDR may also participate in RNA binding, because the YTH domain alone has low affinity for mRNA (Patil *et al.*, 2018). Indeed, the IDR-dependent crosslinks between a YTHDF protein and mRNA detected upon UV-irradiation of living *Arabidopsis* seedlings (Arribas-Hernández et al., 2021a) experimentally supports such a mechanism, conceptually equivalent to the contribution of IDRs in transcription factors to specific DNA binding (Brodsky et al., 2020).

While yeast, flies and primitive land plants encode only one YTHDF protein (Kan et al., 2021; Scutenaire et al., 2018; Scutenaire et al., 2022; Worpenberg et al., 2021), vertebrates have three closely related paralogs (YTHDF1-3) (Patil *et al.*, 2018) and higher plants encode an expanded family, with eleven members in *Arabidopsis* referred to as EVOLUTIONARILY CONSERVED C-TERMINAL REGION1-11 (ECT1-11) (Li et al., 2014a; Ok et al., 2005). It is a question of fundamental importance for the understanding of how complex eukaryotic systems use the regulatory potential of m^6A whether these many YTHDF proteins perform the same biochemical function, or whether they are functionally specialized. Specialization could be driven by i) differential binding specificity to mRNA targets; ii) different molecular

function, perhaps provided by distinct sets of molecular partners or phase-transition properties; and iii) distinct expression patterns or induction by environmental cues, that would result in a diversification of biological functions even if targets and molecular functions are the same.

Initial studies on mammalian cell cultures advocated a model in which YTHDF1 would enhance translation of target mRNAs, YTHDF2 would promote mRNA decay, and YTHDF3 would be able to trigger either of the two (Li et al., 2017; Shi et al., 2017; Wang *et al.*, 2014a; Wang et al., 2015). Nonetheless, recent studies in mouse, zebrafish and human cell culture involving single and combined *ythdf* knockouts and analysis of interacting mRNAs and proteins do not support functional specialization, and propose a unified molecular function for all three vertebrate YTHDFs in accelerating mRNA decay (Kontur et al., 2020; Lasman et al., 2020; Zaccara and Jaffrey, 2020). Such functional redundancy is also supported by structural studies on the YTH domain of the three human paralogs (Li et al., 2020).

The great expansion of YTHDF proteins in higher plants is unique among all other eukaryotes studied. Phylogenetic analyses of plant YTHDF domains have established the existence of 3 clades in angiosperms, DF-A (comprising Arabidopsis ECT1, ECT2, ECT3, ECT4), DF-B (comprising Arabidopsis ECT5, ECT10, ECT9), and DF-C (comprising *Arabidopsis* ECT6, ECT7, ECT8 and ECT11) (Scutenaire *et al.*, 2018). The fact that the eleven *Arabidopsis* paralogs conserve the aromatic residues necessary for specific binding to m^6A (Fray and Simpson, 2015) suggests that they all may function as m^6A readers. The unified model for YTHDF function recently proposed for the three vertebrate paralogs (Kontur *et al.*, 2020; Lasman *et al.*, 2020; Zaccara and Jaffrey, 2020) is consistent with what had already been established for ECT2, ECT3 and ECT4 in the *Arabidopsis* DF-A clade (Arribas-Hernández *et al.*, 2018), even though the three plant paralogs are more divergent in sequence than the highly similar mammalian YTHDF1-3 (Arribas-Hernández *et al.*, 2018; Patil *et al.*, 2018). The two most highly expressed members in Arabidopsis, ECT2 and ECT3, accumulate in dividing cells of organ primordia and exhibit genetic redundancy in the stimulation of stem cell proliferation during organogenesis (Arribas-Hernández *et al.*, 2018; Arribas-Hernández *et al.*, 2020). The two proteins probably act truly redundantly *in vivo* to control this process, because they associate with highly overlapping target sets in wild type plants, and each exhibits increased target mRNA occupancy in the absence of the other protein (Arribas-Hernández *et al.*, 2021b). Simultaneous knockout of *ECT2* and *ECT3* causes a 2-day delay in the emergence of the first true leaves, aberrant leaf morphology, slow root growth and defective root growth directionality among other defects (Arribas-Hernández *et al.*, 2018; Arribas-Hernández *et al.*, 2020) that resemble those of plants with diminished m^6A deposition (Bodi et al., 2012; Růžička et al., 2017; Shen et al., 2016). For the third DF-A clade member, *ECT4*, the genetic redundancy is only noticeable in some

tissues as an exacerbation of *ect2/ect3* phenotypes upon additional mutation of *ect4*, most conspicuously seen in leaf morphogenesis (Arribas-Hernández *et al.*, 2018; Arribas-Hernández *et al.*, 2020). Despite the strong evidence for redundant functions among plant YTHDF paralogs in the DF-A clade, the presence of the many other YTHDF proteins in *Arabidopsis* leaves open the question of whether substantial functional specialization of YTHDF proteins exists in plants.

In this study, we systematically define overlaps in molecular functions of plant YTHDF proteins. Employing a functional assay, we demonstrate that at least one member of all clades in *Arabidopsis*, and the only YTHDF protein from the most basal lineage of land plants, are able to replace ECT2/3/4 function in leaf primordia. In contrast, a few late-diverging ECTs were not able to perform the molecular function of ECT2/3/4. Based on these results, we propose an ancestral molecular role for land plant YTHDF proteins in stimulation of primordial cell proliferation, and sustained functional redundancy during the diversification process that started more than 400 million years ago (Mya). In addition, our results also support the specialization of a small subset of fast-evolving plant YTHDF proteins with contributions to specialization mainly from the IDRs, but also from the YTH domains.

Results

The phylogeny of plant YTHDF proteins comprises more clades than previously estimated

The adaptation of plants to terrestrial life, since the transition from freshwater to land (500-450 Mya) until the rise of angiosperms (~200 Mya), was accompanied by the acquisition of morphological and physiological complexity (Pires and Dolan, 2012). Knowing how diversification of YTHDF proteins came about during the course of plant evolution is relevant to understand their distinct functions, and may hint to roles they might have played in plant evolution. However, the species included in the so far most detailed phylogenetic study on plant YTHDF proteins jump from bryophytes (liverworts and mosses, the first land plants) to angiosperms (flowering plants) (Scutenaire *et al.*, 2018). Therefore, we performed a new phylogenetic analysis using YTHDF proteins from taxa widely spread across plant evolution (Figure 1A). When possible, we included basal clades of each group in addition to model organisms. Because the green alga *Chlamydomonas reinhardtii* lost all YTHDF proteins (Scutenaire *et al.*, 2018), we used *Micromonas pusilla* to represent Chlorophytes. As outgroups we used yeast, fly and mammalian YTHDF proteins, as well as YTHDC proteins that do not contain additional globular domains. The resulting phylogenetic tree largely agrees with the DF-A/B/C clades defined on the basis of angiosperm YTHDF sequences (Scutenaire *et al.*, 2018), but includes some notable differences. The former DF-C group

comprising *Arabidopsis* ECT6/7/8/11 (Scutenaire *et al.*, 2018) can be subdivided into at least two groups that diverged early during YTHDF radiation and are not subtended by a common branch (Figure 1B). Thus, to represent plant YTHDF evolution more accurately, we introduced 'DF-D' for the clade defined by one *Amborella trichopoda* (a basal angiosperm) YTHDF protein, and *Arabidopsis thaliana* ECT6/7 (Figure 1B). We also distinguished between subclades A1/A2 and C1/C2 to reflect early divergences within these clades (Figure 1B). Furthermore, since the group comprising bryophyte YTHDFs did not receive a designation in previous studies, we named it DF-E (for 'Early') (Figure 1B). Finally, an additional group composed of three early-diverging YTHDFs in the fern *Ceratopteris richardii* was named DF-F (for 'Fern'), because they did not fall into any of the other clades (Figure 1B). We conclude that land plant YTHDFs are phylogenetically more diverse than previously appreciated.

YTHDF protein diversification occurred early during land plant evolution

Our phylogenetic analysis shows that plant YTHDF diversification started before the radiation of Euphyllophytes (plants with true leaves comprising ferns, gymnosperms and angiosperms) after their divergence from bryophytes and lycophytes (earliest vascular plants), between 424 and 410 Mya (Magallón et al., 2013). This is because liverworts, mosses and the lycophyte *Selaginella moellendorfii* possess one or two YTHDFs in the 'early clade' (DF-E) while the fern *C. richardii* has six YTHDFs, three of which define the fern-specific DF-F clade and the other three cluster with members of the DF-A or DF-D clades (Figure 1B). On the other hand, the DF-C clade as defined here only diverged in the lineage that gave rise to spermatophytes (seed plants comprising gymnosperms and angiosperms), and the DF-B clade only has members among flowering plants. Thus, our analysis reveals that YTHDF radiation started early in land plant evolution and coincided with the acquisition of morphological complexity and the adaptation to diverse environments.

Functional analysis of plant YTHDF proteins

To address the degree of functional specialization among plant YTHDF proteins in a simple manner, we set up a functional study aimed to determine which YTHDF proteins are able to perform the molecular functions of Arabidopsis ECT2/3/4 that are required for rapid cellular proliferation in leaf primordia. For that purpose, we aimed to express the eleven Arabidopsis *ECT* genes (Figure 2A) in the actively dividing cells where ECT2 and ECT3 are expressed (Arribas-Hernández *et al.*, 2020), and score whether ectopic expression of these YTHDF proteins can suppress the delayed emergence of first true leaves observed in triple *ect2/ect3/ect4* (henceforth, *te234*) mutants (Arribas-Hernández *et al.*, 2018). The most straight-forward approach of using the *ECT2* promoter was not feasible, as pilot experiments

with a genomic *ECT4* fragment revealed that its expression was substantially lower than that of a similar *ECT2* genomic fragment when driven by the *ECT2* promoter (Figure S1), perhaps indicating the presence of internal *cis*-regulatory elements. Thus, the study had to be executed using another promoter active in leaf primordia to drive comparable expression of cDNAs encoding all eleven ECT proteins.

uS7Bp:cECT2-mCherry complements the organogenesis defect of ect2/ect3/ect4

The promoter of the gene *AthuS7B*/*RPS5A* (At3g11940 (Lan et al., 2022)) encoding a ribosomal protein is active in dividing cells (Weijers et al., 2001), similar to the expression domain of ECT2/3/4 (Arribas-Hernández *et al.*, 2018; Arribas-Hernández *et al.*, 2020). We therefore tested whether an *ECT2-mCherry* cDNA fusion expressed under the control of the *AthuS7B* promoter (*uS7Bp*) could complement the delayed leaf formation in *te234* mutants (Figure 2B). Transformation of the *uS7Bp:cECT2-mCherry* construct resulted in complementation frequencies of ~40% among primary transformants, lower but comparable to those obtained with the genomic *ECT2-mCherry* construct under the control of *ECT2* promoter and terminator regions (*ECT2p:gECT2-mCherry*) (Arribas-Hernández et al., 2018, Figure S2A). As control, we used a *uS7Bp:mCherry* construct that showed no complementation (Figure S2A), as expected. Importantly, the leaf morphology and the pattern of mCherry fluorescence in *uS7Bp:cECT2-mCherry* lines was indistinguishable from that of *ECT2p:gECT2-mCherry* (Figure S2B). Hence, we proceeded with expression of cDNAs encoding all of ECT1-11 under the control of the *uS7B* promoter in *te234* mutants.

Percentage of complementation among primary transformants as a readout for functionality

To design the experimental setup, we also considered the fact that expression of transgenes involves severe variations in levels and patterns among transformants. This is due to positional effects of the T-DNA insertion and the propensity of transgenes to trigger silencing in plants (Fagard and Vaucheret, 2000), and explains why only a fraction of *ECT2-mCherry* lines are able to rescue loss of ECT2 function (Figure S2A, (Arribas-Hernández *et al.*, 2018)). Hence, many independent lines need to be analyzed before choosing stable and representative lines for further studies. Taking this into account, we decided to perform systematic and unbiased comparisons on ECT functionality by counting the number of primary transformants (henceforth T1) able to complement the late leaf emergence of *te234* plants (size of first true leaves > 0.5 mm after 10 days of growth) for each construct (Figure S3). To facilitate the interpretation of the results and make transformation batches (experimental repeats) completely comparable, we normalized the percentage of complementing primary transformants to the fraction observed for *uS7Bp:cECT2-mCherry* in each independent transformation (Figure 2C).

Most Arabidopsis YTHDF paralogs can perform the molecular function required for leaf development

The results of the comparative analysis reveal a high degree of functional overlap within the Arabidopsis YTHDF family, because nine out of the eleven YTHDF proteins are able to complement delayed leaf emergence of *ect2/3/4* mutants to some extent, and eight of them do so with a frequency of more than 30% compared to ECT2 when expressed in the same cells (Figure 2C and S4). Importantly, complementation is indirect proof of m^6A-binding ability, because the proteins must bind to the targets whose m^6A-dependent regulation is necessary for correct leaf organogenesis in order to restore ECT2/3/4 function. Thus, most, but not all, Arabidopsis YTHDF proteins retain the molecular function required to stimulate proliferation of primed stem cells.

Hierarchical redundancy among ECT2/3/4

The results of the functional assay for the DF-A clade revealed a clear difference in the degree of complementation by ECT2, ECT3 and ECT4: ECT2 (100%) > ECT3 (83%) > ECT4 (43%). This difference matches the hierarchical redundancy between ECT2/3/4 proteins that we described in previous studies (Arribas-Hernández *et al.*, 2018; Arribas-Hernández *et al.*, 2021b; Arribas-Hernández *et al.*, 2020). However, it remains unclear whether the different importance *in vivo* could be explained only by the different expression levels of the three proteins, as they also follow the same ECT2 > ECT3 > ECT4 ranking (Figure S5), or whether it is related to different ability to perform their common molecular functions. Interestingly, the expression level in the lines selected as best-complementing in our functional study followed a clear ECT4>>ECT3>ECT2 trend (Figure 2D), indicating that ECT4 needs to be overexpressed to perform ECT2/3 function, and that ECT3 needs higher expression than ECT2 to complement to the same extent. Therefore, our results indicate that not only endogenous expression levels, but also molecular functionality may be responsible for the ECT2>ECT3>ECT4 hierarchy. Of note, the agreement between the percentage of T1 plants showing complementation (Figure 2C) and the functional hierarchy between ECT2/3/4, highlights the accuracy with which our functional assay reflects the capacity of the protein to perform the molecular functions required for leaf formation.

Poor ECT2/3/4-like activity of ECT1 and ECT11 IDRs is the main reason for their reduced or absent complementation capacity of te234 plants

Our results suggest that ECT11 and ECT9 are not able to perform the ECT2/3/4 function responsible for leaf formation, and that ECT1 does so only very inefficiently (Figure 2C). Indeed, the two best-complementing *uS7Bp:cECT1-mCherry* lines chosen from the seven

that scored positive in our assay (Figure 2C) only mildly restored leaf shape and growth rate (Figure 3A) despite strong ECT1-mCherry overexpression (Figure 2D). To investigate whether lack of complementation of *te234* plants is due to poor or divergent target-binding affinity by the YTH domain, IDR-related effector functions, or a combination of both, we built chimeric IDR/YTH constructs between ECT2 and ECT1/9/11 (Figure 3B). Additionally, we built an ECT8$_{IDR}$/ECT2$_{YTH}$ chimera (C-8/2) to test whether hybrid constructs can at all be functional, choosing ECT8 as a positive control as it is the highest-scoring ECT (after ECT2) in our functional assay (Figure 2C). Expression of the constructs in *te234* plants showed that chimeras can be, indeed, fully functional, with a complementation score for C-8/2 even higher than ECT2 itself (Figure 3C). ECT1- and ECT11-derived chimeras showed that both the IDR and the YTH domain of the two proteins retain a reduced degree of function compared to the equivalent regions in ECT2 (Figure 3C). However, the IDRs of both proteins scored lower than their YTH domains when combined with the other half from ECT2 (Figure 3C), pointing to the IDR as the main cause for different functionality. In the wild type proteins, the combination of the two poorly-performing halves is likely the cause for the negligible ECT2/3/4-like activity in ECT11 that is only residual in ECT1.

The IDR of ECT9 is incapable of performing ECT2/3/4 molecular functions, but its YTH domain retains some ECT2/3/4-like function

Although the functional study with full-length ECT9 showed no trace of *te234* complementation, we could not conclude that ECT9 lacks ECT2/3/4-like activity, because the transformation efficiency was systematically low over three independent transformations (Figures S3 and S6), allowing the recovery of only 27 lines (Figure 2C) of which only a few exhibited low-level expression (Figure S4) that disappeared in the offspring (second transgenic generation, or T2). However, transformation with ECT9/ECT2-derived chimeras resulted in a low but adequate number of T1s (Figure S7), of which 8% (for C-9/2) and 11% (for C-2/9) exhibited mCherry fluorescence (Figure S8). No complementation capacity was observed for the ECT9-IDR combined with ECT2-YTH domain (C-9/2), while non-zero, albeit low, levels of complementation were observed for the reciprocal C-2/9 construct (Figure 3C). These results show that ECT9 cannot perform the ECT2/3/4-function responsible for the developmental phenotype of *te234* mutants, and point to the IDR as the main site of functional divergence of the protein.

The ability to complement ect2/3/4 does not simply follow affiliation with phylogenetic clades

To extract additional information from the pattern of *ect2/ect3/ect4* complementation by the different YTHDF proteins, we ranked them according to the ability to complement *te234*, again measured as the frequency of fully complementing T1 plants. This property followed

the order ECT2 (100%) > ECT8 (85%) > ECT3 (83%) > ECT5 (60%) > ECT10 (48%) > ECT4 (43%) > ECT7 (39%) > ECT6 (36%) > ECT1 (8%) > ECT11 (0%) = ECT9 (0%) (Figure 2C). Strikingly, the ability to rescue defective timing of leaf emergence did not follow the defined phylogenetic clades, because proteins in the same clades present both the highest and lowest complementation scores, for example ECT8 (85%) vs. ECT11 (0%) in the DF-C clade, and ECT5 (60%) vs. ECT9 (0%) in the DF-B clade (Figures 1B and 2C). Furthermore, the closest homolog to ECT2/3/4 in the DF-A clade, ECT1 (55% amino acid identity to ECT3), showed very poor functional equivalence (Figures 1B and 2C). However, despite the apparent lack of correlation between the functional equivalence and the degree of sequence conservation, it is noteworthy that there is a clear trend for non-complementors to be the most highly divergent proteins in each group, as revealed by the length of the branches in the phylogenetic tree. The reverse is also true: highly complementing proteins have changed less compared to the common ancestor. Indeed, according the phylogenetic trees proposed by us and others (Scutenaire *et al.*, 2018), the shortest branches within each of the DF-A,-B, -C and -D groups belong to the highest-scoring paralogs of each group (ECT2, ECT5, ECT8 and ECT7; blue branches in Figure 1B), while the longest branches correspond to the lowest-scoring paralogs (ECT1, ECT9, ECT11 and ECT6, red branches in Figure 1B). Taken together, these results suggest that the common ancestor of embryophyte YTHDF proteins may have had a molecular function related to that of the modern *Arabidopsis* ECT2/3/4, and that this function has been conserved in the least-divergent members of the DF-A/B/C/D clades after the diversification event that predates angiosperm radiation. Subsequent duplication and neofunctionalization may have driven the rapid evolution of highly-divergent YTHDF proteins in some clades (ECT11, ECT1, and ECT9 in Arabidopsis) that have lost their primary function and perhaps fulfill different molecular roles in the plant m^6A pathway.

The molecular function of ECT2/3/4 was present in the first land plants

To test whether the common ancestor of plant YTHDF proteins had a molecular function similar to that of the modern *Arabidopsis* ECT2/3/4, we subjected the only *Marchantia polymorpha* YTHDF protein (*Mpo*_YTHDF) (Figure 2A) to our functional assay. The result showed a partial, but clear capacity of two different splice forms of *Mpo*_YTHDF to complement the delay in leaf emergence of *Arabidopsis te234* plants (Figures 4A and S9). Furthermore, the leaf morphology defects of *te234* mutants were also partially rescued by the heterologous expression of the liverwort protein (Figures 4B and S10A). Although 4% and 18% complementation scores (for the shorter and longer splice forms respectively) are relatively low, a thorough inspection of the fluorescence intensity in all primary transformants revealed that the transgene was only expressed in a reduced subpopulation, and to low

levels compared to *uS7Bp:cECT2-mCherry* (Figure S10B). This can be due to codon usage bias and propensity to trigger silencing upon heterologous expression of a long cDNA from a distant plant species (Wang and Roossinck, 2006). Therefore, our assay is underestimating the ability of *Mpo*_YTHDF to perform the molecular functions of *Arabidopsis* ECT2/3/4 due to low expression. Nevertheless, the capacity of *Mpo*_YTHDF to complement leaf formation defects caused by a reduced rate of cell proliferation in leaf primordia in Arabidopsis *ect2/ect3/ect4* mutants (Arribas-Hernández *et al.*, 2020) demonstrates that at least part of the molecular activity of *At*_ECT2/3/4 was already present in the first land plants, and suggests that stimulating proliferation of primed stem cells is the ancestral YTHDF molecular function in plants.

Heterologous expression of Human YTHDF2 enhances the phenotype caused by loss of ECT2/3/4 in Arabidopsis

Finally, we tested whether human YTHDF2 (*Hs*_YTHDF2) (Figure 2A) could function molecularly like plant YTHDFs. This question is relevant, because both different and similar molecular mechanisms have been proposed for YTHDF proteins in yeast, plants, invertebrates and vertebrates (Arribas-Hernández and Brodersen, 2020; Kan *et al.*, 2021; Scutenaire *et al.*, 2022; Wang *et al.*, 2014a; Wang *et al.*, 2015; Worpenberg *et al.*, 2021), and even among the three mammalian paralogs (YTHDF1-3) there is no clear consensus as to their molecular functions (Murakami and Jaffrey, 2022). While we did not observe complementation of the delayed leaf emergence or aberrant leaf shape of *te234* plants in any of the 79 transformants expressing *Hs*_YTHDF2-mCherry that we recovered (Figure 5A), several lines showed more acute developmental defects compared to *te234* (Figures 5B and S10B), and some T2 seedlings resembled *Arabidopsis* mutants with severe depletion of m^6A such as *amiR-MTA* (Arribas-Hernández and Brodersen, 2020; Shen *et al.*, 2016). Generally, we observed severe dwarfism and aberrant number and shape of cotyledons and/or first true leaves, although the severity of the phenotype exhibited variable penetrance among T2 siblings for each independent line (Figure 5B). We conclude that expression of *Hs*_YTHDF2 in Arabidopsis *te234* mutants exacerbates its developmental phenotype. This interesting result is in agreement with the generally accepted idea that m^6A/YTHDF2 destabilize mRNA in mammals (Herzog et al., 2017; Ke et al., 2017; Sommer et al., 1978; Wang *et al.*, 2014a; Wang et al., 2014b) while m^6A/ECT2/3/4 do the opposite in plants (Anderson et al., 2018; Arribas-Hernández *et al.*, 2021b; Parker et al., 2020; Shen *et al.*, 2016; Wei et al., 2018). However, an analogous molecular mechanism between plant and mammalian and plant YTHDFs cannot be completely ruled out, because a different cellular context may be hampering the molecular activity of *Hs*_YTHDF2 in plant cells, and

simple competition for targets with remaining ECTs could be the cause of the enhanced phenotype.

Validation of the functional assay by loss-of-function genetic analysis

The results of our functional analysis predict that knockout of genes encoding Arabidopsis YTHDF proteins with ECT2/3/4-like functionality (ECT8 > ECT5 > ECT10 > ECT7 > ECT6) may exacerbate the delay in leaf emergence of *te234* mutants if endogenously expressed in primordial cells. The reverse should also be true: mutation of *ECT1, ECT9* or *ECT11* should not, or in the case of *ECT1* only very slightly, exacerbate the developmental defects of *te234* even if these proteins are naturally expressed in leaf primordia. We chose *ECT1* for validation of this prediction for three reasons. First, mRNA-seq data show that neither the highest-scoring (*ECT8/5*/10) nor the lowest-scoring members (*ECT9/11*) exhibit meristem enrichment (Figure S5). Furthermore, *ECT9/11* are generally very lowly expressed (Figure S5). In contrast, the expression levels and tissue specificity of *ECT1* are comparable to that of *ECT4* (Figure S5) whose activity is easily revealed as an enhancer mutant of *ect2/ect3* (Arribas-Hernández *et al.*, 2018). Second, *ECT1* expression is strong in shoot and root apices as judged by histochemical GUS assays of *Arabidopsis* plants expressing *ECT1p:GUS* (Ok *et al.*, 2005). Third, ECT1 is of particular interest because, as the closest relative of ECT2/3/4 in Arabidopsis, the natural expectation would be some degree of redundancy. Indeed, the considerable expression of *ECT1* in the embryo (Figure S5) may suggest that simultaneous mutation of *ECT1/ECT2/ECT3/ECT4* could phenocopy the embryonic lethality of mutants devoid of a functional methyltransferase complex (Růžička *et al.*, 2017; Shen *et al.*, 2016; Zhong *et al.*, 2008). In this context, the lack of functional redundancy and therefore negligible genetic interaction predicted by our functional assay is not trivial, but rather a challenging concept, and hence appropriate for validation.

ECT1 and ECT2/3/4 are expressed in the same cell types

We first assessed the expression pattern of ECT1 protein using stable transgenic lines expressing a C-terminal TFP-fusion of *ECT1* (*ECT1p:gECT1-FLAG-TFP-ECT1ter*, ECT1-TFP lines, Figure S11A). The pattern of turquoise fluorescence was strongly reminiscent of that of fluorescent ECT2/3/4 fusions (Arribas-Hernández *et al.*, 2018) with signal at the base of young leaves, in leaf primordia, main root tips and lateral root primordia at different stages (Figure 6A-D). Thus, the overlap in ECT1 and ECT2/3/4 expression patterns is substantial. We note that these transgenic lines selected on the basis of visible and reproducible pattern of fluorescence may have elevated expression levels compared to the endogenous *ECT1*, because we could detect *ECT1-TFP* mRNA but not the endogenous transcript by RNA blotting (Figure S11B).

ECT1 resides in the cytoplasm where it can form granules

To perform ECT2/3/4-like functions, ECT1 would also need to be cytoplasmic. Confocal microscopy of meristematic root cells indeed showed cytoplasmic signal with heterogenous texture similar to what we previously described for ECT2/3/4 (Arribas-Hernández *et al.*, 2018) (Figure 6E). However, most roots had a few cells containing distinct ECT1-TFP foci (Figure 6F) that formed in the absence of stress-inducing treatments like heat or drought that have been used to induce granule formation by ECT2/3/4 (Arribas-Hernández *et al.*, 2018; Scutenaire *et al.*, 2018). Importantly, we found no trace of free TFP that could be causing artifacts in the imaging (Figure S11A). We conclude from the similar expression pattern and subcellular localization of ECT1 and ECT2/3/4 that assessment of the possible exacerbation of *te234* phenotypes by additional loss of *ECT1* function is a meaningful test of our functional assay.

Mutation of ECT1 does not exacerbate the phenotype of ect2/ect3/ect4 plants

We isolated three lines homozygous for T-DNA insertions in the *ECT1* gene body, *ect1-1* (SAIL_319_A08), *ect1-2* (GK-547H06), and *ect1-3* (SALK_059722) (Figure 6G) and, based on qPCR analyses, concluded that the three are knockout mutations (Figure 6H). We used the *ect1-1* and *ect1-2* alleles for subsequent systematic genetic analyses with a series of single, double, triple and quadruple mutants of *ect1* combined with *ect2*, *ect3* and *ect4*. Importantly, both *ect1-1/ect2-1/ect3-1/ect4-2 (qe1234*, for 'quadruple *ect1/2/3/4*', see Figure S11C for multiple mutant abbreviations) and *ect1-2/ect2-3/ect3-2/ect4-2* (*Gqe1234*, for 'GABI-KAT quadruple *ect1/2/3/4*') mutant plants were viable, excluding the possibility that mutants lacking the complete DF-A clade phenocopy the lethality of m^6A-deficient mutants (Zhong *et al.*, 2008). Furthermore, the timing of the leaf emergence and the overall rosette morphology were indistinguishable from the corresponding *te234* and *Gte234* parental mutants (Figure 6I and S11D). Similarly, *ect1-2/ect2-3/ect3-2* (*Gte123*) mutants were identical to *ect2-3/ect3-2 (Gde23)*, and single *ect1* mutants did not show any obvious defects (Figure 6I and S11D). Additional analysis of trichome branching and root morphology did not detect defects caused by mutation of *ECT1* in any background tested (Figure S11E,F). Thus, the thorough genetic analysis undertaken here did not reveal any indication of redundancy between ECT1 and the other three DF-A clade proteins, despite the fact that ECT1 is expressed in a pattern similar to that of the other DF-A paralogs. This conclusion is in agreement with the poor ECT2/3/4-like activity shown by ECT1 in our functional assays, thereby validating the approach.

Discussion

Functional versus biological redundancy

Our study reveals that most YTHDF proteins in higher plants can perform, essentially, the same molecular function. We anticipate that this molecular function is used in specific biological contexts by ECT8/5/10/7/6 due to different expression patterns and response to stimuli, thereby achieving biological specialization with respect to ECT2/3/4. Such variability can already be inferred from available RNA-Seq data that show, for example, ECT8 to be primarily expressed during senescence-associated processes (http://bar.utoronto.ca/efp2/Arabidopsis/Arabidopsis_eFPBrowser2.html). In addition to redundancy, there is a clear pattern of lineage-specific specialization in fast-evolving YTHDF proteins from different clades, exemplified in Arabidopsis by ECT1, ECT11 and ECT9. Whether these proteins act to counteract the ECT2/3/4-like function by binding-competition to m^6A-containing transcripts, perhaps halting growth upon stress, or whether they perform independent functions in different tissues or cell types, is open for new investigations.

ECT1 is a newly evolved gene in a Brassicaceae lineage

Surprisingly, the only member of the DF-A clade not yet characterized as m^6A reader, ECT1, scored low in our functional assay and indeed, inactivation of *ECT1* does not enhance the phenotype caused by loss of *ECT2/3/4* despite expression of *ECT1* in the same cell types and subcellular compartment as the other DF-A paralogs. We note that a previous description of nuclear and cytoplasmic fluorescence of a *35Sp:ECT1-GFP* fusion (Ok *et al.*, 2005) may be due to the fact that the authors used epifluorescence instead of confocal fluorescence microscopy for the analyses. Because that technique does not distinguish between inside or around the nucleus, the signal observed may have been perinuclear, e.g. from the endoplasmic reticulum. But then, why is ECT1 so similar in sequence, yet so different functionally? A thorough look at phylogenetic analyses from Scutenaire *et al.* (2018) reveals that *ECT1* is only present in species of the 'lineage I' of Brassicaceae such as *A. thaliana* and *Capsella rubella* (Nikolov et al., 2019). The closely related *Brassica oleracea* ('lineage II') (Nikolov *et al.*, 2019) has a clear homolog of *Ath/Cru ECT3*, but not *ECT1* (Scutenaire *et al.*, 2018), while other dicots outside *Brassicaceae* encode *ECT3/1* orthologs in a separate cluster (Scutenaire *et al.*, 2018). Therefore, *ECT1* is the product of a recent duplication and neofunctionalization event of the *ECT3/1* gene in a lineage of *Brassicaceae* that diverged more rapidly than any other DF-A2 clade member in *Arabidopsis* (Figure 1B, (Scutenaire *et al.*, 2018)). This is in agreement with our overall conclusion that most YTHDFs in early angiosperms possessed *Mpo*_YTHDF/*Ath*_ECT2/3/4 molecular functions, and only late diverging events resulted in specialization of a few YTHDF proteins. For ECT1, such duplication and neofunctionalization event occurred late in a small subgroup of dicots. We note that such rapid neofunctionalization appears to result primarily from changes in the

IDR. This observation underscores the urgent need to understand the functional elements of the IDR that endow YTHDF proteins with specific functions. It also hints that comparative analysis of pairs of YTHDF proteins such as ECT1/ECT3 that are closely related in sequence, but divergent in function could be of considerable value in this regard.

DF-A proteins evolved fast during the rapid diversification of angiosperms

Our phylogenetic analysis reveals that the DF-A clade originated before the divergence of ferns from the ancestor of seed plants, at least 410 Mya (Magallón *et al.*, 2013) but two clear branches, DF-A1 and DF-A2, emerge from a clear common stem (Figure 1B). While DF-A1 contains early-diverging DF-A proteins in ferns, gymnosperms, and the basal angiosperm *Amborella trichopoda*, the second group (DF-A2) is subtended by a long branch that comprises the only *Nymphaea colorata* DF-A and all monocot and dicot DF-A proteins (Figure 1B). Because *Amborellaceae* and *Nymphaeaceae* (water lilies) are sister groups to all other angiosperms (Figure 1A), the result suggests that the DF-A protein present in the most recent common ancestor of all extant angiosperms underwent a period of rapid evolution in a narrow window of time at the onset of the great angiosperm expansion (Soltis et al., 2008). Because it is clear that the DF-A members ECT2/3/4 play an important role in the development of current dicots, it is tempting to speculate whether this rapid change in the ancestral DF-A protein could be connected to angiosperm evolution.

The diversity of plant YTHDF proteins and the need for many YTHDFs in complex plants

Ferns diverged from other vascular plants ~400 Mya, around the same time that early tetrapods evolved from fish. While the observation that a few fern YTHDF proteins cluster in DF-A and -C clades points to an early diversification of plant YTHDFs, the fact that the other half of the *C. richardii* YTHDF repertoire defines an independent clade (DF-F) suggests that complex plants may need many different YTHDFs, well surpassing the three paralogs found in most vertebrates (Patil *et al.*, 2018). But why? The need for many YTHDFs of considerable variability is all the more puzzling given our demonstration here that the majority of them retains the same molecular function. Robustness is a commonly given explanation for redundancy, but the same argument could apply to methyltransferase subunits, and *Arabidopsis* has maintained only one copy of *MTA*, *MTB*, *FIP37*, *VIR* and *HAKAI* (Balacco and Soller, 2019). Therefore, the answer should probably be sought elsewhere. It is clear now that the m^6A/YTHDF axis controls cellular proliferation and organ growth in plants (Arribas-Hernández and Brodersen, 2020; Arribas-Hernández *et al.*, 2020), and a principal difference between animals and plants is the extreme plasticity of plant growth. Because growth and stress responses are also tightly intertwined, it is possible that plants use a plethora m^6A-YTHDF growth-stimulators in different organs, responsive to

different stresses and developmental cues, to shape plant architecture in response to stimuli. The answer to the paradox may be in the details: plant YTHDFs responsive to different environmental cues may fine-tune growth programs through slightly different performance and target-binding capacity in partly overlapping expression domains, where they are known to compete for targets (Arribas-Hernández *et al.*, 2021b).

Acknowledgements

We thank Lena Bjørn Johansson, Sergio D'Anna and Tobias Lahti for technical assistance, and Theo Bølsterli and his team for plant care. We acknowledge the constructive criticism of Rupert Fray as a reviewer on previous publications as his suggestion to use the *ect2/ect3/ect4* triple mutant phenotype to test ECT molecular function by systematic ectopic expression in the ECT2 expression domain inspired us to embark on the present project. This work was supported by a Hallas-Møller Ascending Investigator 2019 grant (NNF19OC0054973) from the Novo Nordisk Foundation and by a Research Project2 grant (9040-00409B) from the Independent Research Fund Denmark to P.B.

Materials and Methods

Plant material and growth conditions

All the used lines are in the *A. thaliana* Columbia-0 (Col-0) ecotype. The T-DNA insertion lines *ect1-1* (SAIL_319_A08), *ect1-2* (GK-547H06), and *ect1-3* (SALK_059722) were obtained from Nottingham Arabidopsis Stock Centre. The mutants *ect2-3*, *ect3-2*, *ect2-3/ect3-2* (*Gde23*), *ect2-3/ect3-2/ect4-2* (*Gte234*) and *ect2-1/ect3-1/ect4-2* (*te234*), used for genetic crosses to *ect1* alleles or for background to produce transgenic lines, have been previously described (Arribas-Hernández *et al.*, 2018; Arribas-Hernández *et al.*, 2020).

For *in vitro* growth, seeds were sterilized by consecutive incubation in 70 % EtOH (2 min) and [1.5 % NaClO, 0.05 % Tween-20] (10 min) followed by two washes with sterile Milli-Q H_2O, and spread on petri dishes containing Murashige & Skoog (MS) media (4.4 g/L salt mixture, 10 g/L sucrose, 8 g/L agar) supplemented with the appropriate antibiotics. Following 2-5 days of stratification at 4C in darkness, the plates were transferred to incubators at 21° C in long day conditions (16h-light/8h-dark photoperiod, 120 µmol m^{-2} s^{-1} light intensity). When further growth was needed, plants were transferred to soil and grown in incubators with the same conditions for phenotypic characterization, or standard greenhouse facilities for seed production.

Phylogenetic analysis

Sequences of selected YTH-domain-containing proteins were downloaded from UniProt (Apweiler et al., 2004), TAIR (www.arabidopsis.org), phytozome (Goodstein et al., 2012) or

GinkgoDB (Gu et al., 2022) and aligned with Clustal Omega (Sievers et al., 2011) webserver (https://www.ebi.ac.uk/Tools/msa/clustalo/) with default parameters. Evolutionary analyses were conducted in MEGA7 (Kumar et al., 2016). The phylogenetic tree was generated from the alignment (Supplemental Dataset 1) using the neighbor-joining method (Saitou and Nei, 1987). Values of the bootstrap test (Felsenstein, 1985) were inferred from 1000 replicates. The evolutionary distances were computed using the Poisson correction method (Zuckerkandl and Pauling, 1965) and are in the units of the number of amino acid substitutions per site.

Cloning

We employed the scar-free USER cloning method (Bitinaite and Nichols, 2009) to produce all *uS7Bp:cYTHDF(X)-mCherry-OCSter* constructs by gluing four DNA fragments (*uS7Bpro*, *cYTHDF(X), mCherry, OCSter*) into the pCAMBIA3300-U plasmid (Nour-Eldin et al., 2006). The cloning strategy is analogous to the one described for the *ECT2p:gECT2-mCherry-ECT2ter* construct (Arribas-Hernández *et al.*, 2018). This plasmid was also used as a template to PCR-amplify the *mCherry* sequence. *uS7Bpro* and *OCSter* fragments were amplified from the GreenGate Cloning System (Addgene) plasmids pGGA012 and pGGF005 respectively (Lampropoulos et al., 2013). The specific fragments containing cDNA of the different YTHDF proteins (*cYTHDF(X)*) were amplified from commercial plasmids containing the cDNA clone of interest or, when unavailable, we used reverse-transcribed cDNA from RNA (see below). A list with all the templates used to amplify cDNA and the specific transcript isoform contained in the resulting constructs can be found in Supplemental Table 1. We designed the U-containing USER-primers in a way that the same three PCR fragments common to all constructs (*uS7Bpro*, *mCherry*, and *OCSter*) could be used in all ligations, and only the fragment encoding the cYTHDF gene had to be customized. For the chimeras, the strategy was comparable but gluing only two fragments: *uS7Bp:cIDR*$_{YTHDF(X)}$ and *cYTH*$_{YTHDF(Y)}$*-mCherry-OCSter*, amplified from the previously obtained *uS7Bp:cYTHDF(X)-mCherry-OCSter* and *uS7Bp:cYTHDF(Y)-mCherry-OCSter* constructs.

The construction of *ECT1p:gECT1-FLAG-TFP-ECT1ter* was done by USER cloning (Bitinaite and Nichols, 2009) using gDNA from Arabidopsis tissues to amplify the *ECT1* gene body and regulatory sequences, in identical way than described for *ECT2* in the construction of *ECT2p:gECT2-mCherry-ECT2ter* (Arribas-Hernández *et al.*, 2018). A plasmid containing *MTAp:gMTA-FLAG-TFP-MTAter* (Arribas-Hernández *et al.*, 2020) was used as template to amplify the FLAG-TFP fragment.

Cloning of the trial *ECT2p:gECT1-mCherry-ECT2ter* and *ECT2p:gECT4-mCherry-ECT2ter* constructs was done by GreenGate (Lampropoulos *et al.*, 2013). In short, PCR fragments were amplified by PCR using Thermo Scientific Phusion High-Fidelity DNA Polymerase

(NEB) and introduced into entry vectors by BsaI-restriction cloning, as specified in Supplemental Table 2. Of note, because none of our constructs carried an N-tag (fragment B-C), the fragment containing *ECT1/4* gDNA (from ATG to the last codon prior stop) was cloned using primers with B-to-D overhangs into pGEM-T Easy by A-tailing (Promega), thereby bypassing the need of a B-C element. The vectors containing the *ECT2* 5'UTR and upstream regulatory sequences (in pGGA000), the coding sequences (as gDNA) of *ECT1/4* (in pGEM-T Easy), linker-mCherry (pGGD003), the *ECT2* 3'UTR and downstream sequences (in pGGE000) and the D-AlaR cassette (pGGF003) were combined in a 'Greengate reaction' using BsaI-HF (NEB), T4 DNA-Ligase (Thermo Scientific) and pGGZ001 as destination vector (Lampropoulos *et al.*, 2013). All vectors were obtained from addgene (plasmid kit #1000000036).

In all cases, the constructs were introduced into DH5α competent *Escherichia coli* cells (New England Biolabs) and Sanger-sequenced to discard clones with PCR-derived mutations. A list containing the sequences of all cloning primers, the fragments obtained with every primer set, and how these fragments were combined in the different constructs, can be found in Supplemental Table 2.

Plant transformation and line selection

All final binary plasmids were introduced into *Agrobacterium tumefaciens* GV3101 to transform the appropriate plants (specified below) by floral dipping (Clough and Bent, 1998). *ECT1p:gECT1-TFP-ECT1ter* lines in the *ect1-2* background were selected on large MS-agar plates containing glufosinate ammonium (10 mg/L) for selection, and ampicillin (100 mg/L) to prevent *Agrobacterium* growth. Resistant primary transformants were transferred to soil at ~9 days after germination. For line selection, T2 seedlings were screened for single insertions according to the segregation of glufosinate-resistance, and visible fluorescence in a consistent pattern among many lines. Absence of free TFP was assessed by western blot, performed as described by Arribas-Hernández et al. (2018).

ECT2p:gECT1-ECT2ter and *ECT2p:gECT1-ECT2ter* primary transformants in the *te234* background were selected in a similar manner but using 3 mM D-Alanine for selection.

The analysis of *uS7Bp:cYTHDF(X)-mCherry-OCSter* constructs and derived chimeras in *te234* plants for the functional assay is detailed below.

Complementation assay

Due to the large amount of constructs tested, and the practical impossibility of simultaneous transformation of all constructs at once in our facilities, we performed repeated transformations of subsets of constructs to be compared, ensuring that each protein had at

least two independent transformations done in parallel with the *uS7Bp:cECT2-mCherry-OCSter* and *uS7p:mCherry-OCSter* controls. The constructs dipped in each parallel transformation can be found in Figures S3 (*Arabidopsis* ECTs), S7 (ECT-chimeras) and S9 (*Marchantia* and human YTHDFs). To even out the inevitable pot-to-pot differences in transformation efficiency, we dipped between 2 and 4 pots, with 4-6 plants per pot, for each construct in every transformation, and harvested the seeds from different pots individually. To measure complementation, T1 seeds were sterilized and spread on large (135 mm) petri dishes (~2000 seeds (100 µL) / plate) containing MS-agar media supplemented with glufosinate ammonium (10 mg/L), sulfadiazine (4.83 mg/L) and ampicillin (100 mg/L). On average, we observed transformation efficiencies of ~0.8% (~15.3 transformants per plate) with roughly comparable values among constructs and transformation batches except for *ECT9* and *Hs_YTHDF2*, for which we obtained a consistently lower amount of transformants (Figure S6). Based on the transformation efficiency obtained in a first pilot transformation batch with only ECT2 and the mCherry control (Figures S2 and S6), we standardized a minimum of six plates per construct to be assessed in parallel in every independent assay, aiming to have >100 T1s of each type in any given independent comparison. Among the set of plates of each construct, we included repeats of the 2-4 independent seed batches originated from separate pots.

The seeds were stratified, germinated and grown as described above. Complementation was scored after 10 days of parallel growth for all genotypes included in the same batch. We considered seedlings with first true leaves of >0.5 mm (basal-to-apical length) as 'complementing', and those of inferior size as 'not complementing'. Complementation percentage for each construct in every batch was then calculated as the ratio between the number of complementing seedlings and the total amount of transformants (x100%) normalized to the percentage of complementing T1s for ECT2 in the same batch. The final score given to each construct in Figures 2C, 3C, 4A and 5A is the average of the complementation percentages in all batches for which the construct was present, weighted by the amount of primary transformants recovered for that construct in each batch. For each score, the total amount of transformants (n) and independent transformations (I.T.) is indicated, and the raw numbers can be found in Figures S3, S7 and S9.

Genotypic and phenotypic characterization

DNA extraction and genotyping of *ect1, ect2, ect3* and *ect4* alleles for the construction of high order mutants, photographs of rosettes and seedlings, root growth characterization, and quantification of trichome branching were done with the same way and with the same equipment as described previously (Arribas-Hernández *et al.*, 2018; Arribas-Hernández *et*

al., 2020). The sequences of *ECT1*-specific primers not used in the 2018 study can be found in the Supplemental Table 2.

Fluorescence microscopy

Stereo and confocal fluorescence microscopy were performed using the same equipment and methodology than Arribas-Hernández et al. (2020)

cDNA obtention

cDNA was obtained using total RNA from *A. thaliana* Col-0 wild type flowers, dissected gemma cups and apical notches *of M. polymorpha* that grows spontaneously in humid areas of our greenhouses, or human HepG2 cells (Sigma 85011430). In all cases, the RNA was extracted using trizol, and reverse transcribed with oligo-dT primers to produce cDNA as previously described (Arribas-Hernández *et al.*, 2018).

Quantitative PCR

Quantitative real-time RT-PCR was performed on the Bio-Rad CFX ConnectTM thermal cycler using the QuantiTect SYBR Green RT-PCR kit (Qiagen) following the instructions from the manufacturer. Expression analysis was performed following the $\Delta\Delta C\#$ method (Pfaffl, 2001). Samples were run in quadruplicates, and relative expression levels were normalized to *ACTIN* (AT3G18780) as housekeeping gene. A list of qPCR primers can be found in Supplemental Table 2.

Northern blot

Northern blot to detect *ECT1* mRNA from total RNA of Arabidopsis flowers was performed as described previously for *ECT2* and *ECT3* (Arribas-Hernández *et al.*, 2018). Primer sequences for the *ECT1*-specific probe are detailed in Supplemental Table 2.

References

Anderson, S.J., Kramer, M.C., Gosai, S.J., Yu, X., Vandivier, L.E., Nelson, A.D.L., Anderson, Z.D., Beilstein, M.A., Fray, R.G., Lyons, E., and Gregory, B.D. (2018). N(6)-Methyladenosine Inhibits Local Ribonucleolytic Cleavage to Stabilize mRNAs in Arabidopsis. Cell Rep. *25*, 1146-1157. 10.1016/j.celrep.2018.10.020.

Arribas-Hernández, L., Bressendorff, S., Hansen, M.H., Poulsen, C., Erdmann, S., and Brodersen, P. (2018). An m6A-YTH Module Controls Developmental Timing and Morphogenesis in Arabidopsis. Plant Cell *30*, 952-967.

Arribas-Hernández, L., and Brodersen, P. (2020). Occurrence and functions of m6A and other covalent modifications in plant mRNA. Plant Physiol. *182*, 79-96. 10.1104/pp.19.01156.

Arribas-Hernández, L., Rennie, S., Köster, T., Porcelli, C., Lewinski, M., Dr. Dorothee Staiger, P., Andersson, R., and Brodersen, P. (2021a). Principles of mRNA targeting via the Arabidopsis m6A-binding protein ECT2. eLife *10*, e72375. 10.7554/eLife.72375.

Arribas-Hernández, L., Rennie, S., Schon, M., Porcelli, C., Enugutti, B., Andersson, R., Nodine, M.D., and Brodersen, P. (2021b). The YTHDF proteins ECT2 and ECT3 bind largely overlapping target sets and influence target mRNA abundance, not alternative polyadenylation. eLife *10*, e72377. 10.7554/eLife.72377.

Arribas-Hernández, L., Simonini, S., Hansen, M.H., Paredes, E.B., Bressendorff, S., Dong, Y., Østergaard, L., and Brodersen, P. (2020). Recurrent requirement for the m6A-ECT2/ECT3/ECT4 axis in the control of cell proliferation during plant organogenesis. Development *147*, dev189134. 10.1242/dev.189134.

Balacco, D.L., and Soller, M. (2019). The m6A Writer: Rise of a Machine for Growing Tasks. Biochemistry *58*, 363-378. 10.1021/acs.biochem.8b01166.

Bitinaite, J., and Nichols, N.M. (2009). DNA cloning and engineering by uracil excision. Curr. Protoc. Mol. Biol. *Chapter 3*, Unit 3 21. 10.1002/0471142727.mb0321s86.

Bodi, Z., Zhong, S., Mehra, S., Song, J., Graham, N., Li, H., May, S., and Fray, R.G. (2012). Adenosine methylation in Arabidopsis mRNA is associated with the 3' end and reduced levels cause developmental defects. Front. Plant Sci. *3*, 48. 10.3389/fpls.2012.00048.

Boo, S.H., Ha, H., Lee, Y., Shin, M.-K., Lee, S., and Kim, Y.K. (2022). UPF1 promotes rapid degradation of m6A-containing RNAs. Cell Rep. *39*, 110861. https://doi.org/10.1016/j.celrep.2022.110861.

Brodsky, S., Jana, T., Mittelman, K., Chapal, M., Kumar, D.K., Carmi, M., and Barkai, N. (2020). Intrinsically Disordered Regions Direct Transcription Factor In Vivo Binding Specificity. Mol. Cell *79*, 459-471.e454. 10.1016/j.molcel.2020.05.032.

Clough, S.J., and Bent, A.F. (1998). Floral dip: a simplified method for Agrobacterium-mediated transformation of Arabidopsis thaliana. Plant J. *16*, 735-743. 10.1046/j.1365-313x.1998.00343.x.

Du, H., Zhao, Y., He, J., Zhang, Y., Xi, H., Liu, M., Ma, J., and Wu, L. (2016). YTHDF2 destabilizes m6A-containing RNA through direct recruitment of the CCR4–NOT deadenylase complex. Nat. Commun. *7*, 12626. 10.1038/ncomms12626 https://www.nature.com/articles/ncomms12626#supplementary-information.

Fagard, M., and Vaucheret, H. (2000). (TRANS)GENE SILENCING IN PLANTS: How Many Mechanisms? Annu. Rev. Plant Physiol. Plant Mol. Biol. *51*, 167-194. 10.1146/annurev.arplant.51.1.167.

Felsenstein, J. (1985). Confidence Limits on Phylogenies: An Approach Using the Bootstrap. Evolution *39*, 783-791. 10.2307/2408678.

Fray, R.G., and Simpson, G.G. (2015). The Arabidopsis epitranscriptome. Curr. Opin. Plant Biol. *27*, 17-21. http://dx.doi.org/10.1016/j.pbi.2015.05.015.

Geula, S., Moshitch-Moshkovitz, S., Dominissini, D., Mansour, A.A., Kol, N., Salmon-Divon, M., Hershkovitz, V., Peer, E., Mor, N., Manor, Y.S., et al. (2015). m6A mRNA methylation facilitates resolution of naïve pluripotency toward differentiation. Science *347*, 1002-1006. 10.1126/science.1261417.

Goodstein, D.M., Shu, S., Howson, R., Neupane, R., Hayes, R.D., Fazo, J., Mitros, T., Dirks, W., Hellsten, U., Putnam, N., and Rokhsar, D.S. (2012). Phytozome: a comparative platform for green plant genomics. Nucleic Acids Res. *40*, D1178-D1186. 10.1093/nar/gkr944.

Gu, K.-J., Lin, C.-F., Wu, J.-J., and Zhao, Y.-P. (2022). GinkgoDB: an ecological genome database for the living fossil, Ginkgo biloba. Database *2022*, baac046. 10.1093/database/baac046.

Herzog, V.A., Reichholf, B., Neumann, T., Rescheneder, P., Bhat, P., Burkard, T.R., Wlotzka, W., von Haeseler, A., Zuber, J., and Ameres, S.L. (2017). Thiol-linked alkylation of RNA to assess expression dynamics. Nat. Meth. *14*, 1198. 10.1038/nmeth.4435 https://www.nature.com/articles/nmeth.4435#supplementary-information.

Kan, L., Ott, S., Joseph, B., Park, E.S., Dai, W., Kleiner, R.E., Claridge-Chang, A., and Lai, E.C. (2021). A neural m6A/Ythdf pathway is required for learning and memory in Drosophila. Nat. Commun. *12*, 1458. 10.1038/s41467-021-21537-1.

Ke, S., Pandya-Jones, A., Saito, Y., Fak, J.J., Vågbø, C.B., Geula, S., Hanna, J.H., Black, D.L., Darnell, J.E., and Darnell, R.B. (2017). m6A mRNA modifications are deposited in nascent pre-mRNA and are not required for splicing but do specify cytoplasmic turnover. Genes Dev. *31*, 990-1006.

Kontur, C., Jeong, M., Cifuentes, D., and Giraldez, A.J. (2020). Ythdf m6A Readers Function Redundantly during Zebrafish Development. Cell Rep. *33*, 108598. https://doi.org/10.1016/j.celrep.2020.108598.

Kumar, S., Stecher, G., and Tamura, K. (2016). MEGA7: Molecular Evolutionary Genetics Analysis Version 7.0 for Bigger Datasets. Mol. Biol. Evol. *33*, 1870-1874. 10.1093/molbev/msw054.

Lampropoulos, A., Sutikovic, Z., Wenzl, C., Maegele, I., Lohmann, J.U., and Forner, J. (2013). GreenGate - A Novel, Versatile, and Efficient Cloning System for Plant Transgenesis. PLOS ONE *8*, e83043. 10.1371/journal.pone.0083043.

Lan, T., Xiong, W., Chen, X., Mo, B., and Tang, G. (2022). Plant cytoplasmic ribosomal proteins: an update on classification, nomenclature, evolution and resources. Plant J. *110*, 292-318. https://doi.org/10.1111/tpj.15667.

Lasman, L., Krupalnik, V., Viukov, S., Mor, N., Aguilera-Castrejon, A., Schneir, D., Bayerl, J., Mizrahi, O., Peles, S., Tawil, S., et al. (2020). Context-dependent functional compensation between Ythdf m6A reader proteins. Genes Dev. *34*, 1373-1391.

Li, A., Chen, Y.-S., Ping, X.-L., Yang, X., Xiao, W., Yang, Y., Sun, H.-Y., Zhu, Q., Baidya, P., Wang, X., et al. (2017). Cytoplasmic m6A reader YTHDF3 promotes mRNA translation. Cell Res. *27*, 444. 10.1038/cr.2017.10 https://www.nature.com/articles/cr201710#supplementary-information.

Li, D., Zhang, H., Hong, Y., Huang, L., Li, X., Zhang, Y., Ouyang, Z., and Song, F. (2014a). Genome-wide identification, biochemical characterization, and expression analyses of the YTH domain-containing RNA-binding protein family in Arabidopsis and rice. Plant Mol. Biol. Report. *32*, 1169-1186. 10.1007/s11105-014-0724-2.

Li, F., Zhao, D., Wu, J., and Shi, Y. (2014b). Structure of the YTH domain of human YTHDF2 in complex with an m6A mononucleotide reveals an aromatic cage for m6A recognition. Cell Res. *24*, 1490-1492. 10.1038/cr.2014.153.

778 Li, Y., Bedi, R.K., Moroz-Omori, E.V., and Caflisch, A. (2020). Structural and Dynamic Insights into
779 Redundant Function of YTHDF Proteins. Journal of Chemical Information and Modeling *60*, 5932-
780 5935. 10.1021/acs.jcim.0c01029.

781 Liu, N., Dai, Q., Zheng, G., He, C., Parisien, M., and Pan, T. (2015). N6-methyladenosine-dependent
782 RNA structural switches regulate RNA-protein interactions. Nature *518*, 560-564.
783 10.1038/nature14234.

784 Luo, S., and Tong, L. (2014). Molecular basis for the recognition of methylated adenines in RNA by
785 the eukaryotic YTH domain. Proc. Natl. Acad. Sci. USA *111*, 13834-13839.
786 10.1073/pnas.1412742111.

787 Magallón, S., Hilu, K.W., and Quandt, D. (2013). Land plant evolutionary timeline: Gene effects are
788 secondary to fossil constraints in relaxed clock estimation of age and substitution rates. Am. J. Bot.
789 *100*, 556-573. https://doi.org/10.3732/ajb.1200416.

790 Murakami, S., and Jaffrey, S.R. (2022). Hidden codes in mRNA: Control of gene expression by m6A.
791 Mol. Cell *82*, 2236-2251. https://doi.org/10.1016/j.molcel.2022.05.029.

792 Nikolov, L.A., Shushkov, P., Nevado, B., Gan, X., Al-Shehbaz, I.A., Filatov, D., Bailey, C.D., and
793 Tsiantis, M. (2019). Resolving the backbone of the Brassicaceae phylogeny for investigating trait
794 diversity. New Phytol. *222*, 1638-1651. https://doi.org/10.1111/nph.15732.

795 Nour-Eldin, H.H., Hansen, B.G., Norholm, M.H., Jensen, J.K., and Halkier, B.A. (2006). Advancing
796 uracil-excision based cloning towards an ideal technique for cloning PCR fragments. Nucleic Acids
797 Res. *34*, e122. 10.1093/nar/gkl635.

798 Ok, S.H., Jeong, H.J., Bae, J.M., Shin, J.S., Luan, S., and Kim, K.N. (2005). Novel CIPK1-associated
799 proteins in Arabidopsis contain an evolutionarily conserved C-terminal region that mediates nuclear
800 localization. Plant Physiol. *139*, 138-150. 10.1104/pp.105.065649.

801 Park, O.H., Ha, H., Lee, Y., Boo, S.H., Kwon, D.H., Song, H.K., and Kim, Y.K. (2019).
802 Endoribonucleolytic Cleavage of m6A-Containing RNAs by RNase P/MRP Complex. Mol. Cell *74*,
803 494-507.e498. https://doi.org/10.1016/j.molcel.2019.02.034.

804 Parker, M.T., Knop, K., Sherwood, A.V., Schurch, N.J., Mackinnon, K., Gould, P.D., Hall, A.J.W.,
805 Barton, G.J., and Simpson, G.G. (2020). Nanopore direct RNA sequencing maps the complexity of
806 Arabidopsis mRNA processing and m6A modification. eLife *9*, e49658. 10.7554/eLife.49658.

807 Patil, D.P., Pickering, B.F., and Jaffrey, S.R. (2018). Reading m6A in the Transcriptome: m6A-Binding
808 Proteins. Trends Cell Biol. *28*, 113-127. 10.1016/j.tcb.2017.10.001.

809 Pfaffl, M.W. (2001). A new mathematical model for relative quantification in real-time RT–PCR.
810 Nucleic Acids Res. *29*, e45-e45.

811 Pires, N.D., and Dolan, L. (2012). Morphological evolution in land plants: new designs with old genes.
812 Philosophical Transactions of the Royal Society B: Biological Sciences *367*, 508-518.
813 10.1098/rstb.2011.0252.

814 Růžička, K., Zhang, M., Campilho, A., Bodi, Z., Kashif, M., Saleh, M., Eeckhout, D., El-Showk, S., Li,
815 H., Zhong, S., et al. (2017). Identification of factors required for m6A mRNA methylation in
816 Arabidopsis reveals a role for the conserved E3 ubiquitin ligase HAKAI. New Phytol. *215*, 157-172.
817 10.1111/nph.14586.

818 Saitou, N., and Nei, M. (1987). The neighbor-joining method: a new method for reconstructing
819 phylogenetic trees. Mol. Biol. Evol. *4*, 406-425. 10.1093/oxfordjournals.molbev.a040454.

820 Scutenaire, J., Deragon, J.-M., Jean, V., Benhamed, M., Raynaud, C., Favory, J.-J., Merret, R., and
821 Bousquet-Antonelli, C. (2018). The YTH Domain Protein ECT2 Is an m6A Reader Required for
822 Normal Trichome Branching in Arabidopsis. Plant Cell *30*, 986-1005. 10.1105/tpc.17.00854.

Scutenaire, J., Plassard, D., Matelot, M., Villa, T., Zumsteg, J., Libri, D., and Séraphin, B. (2022). The S. cerevisiae m⁶A-reader Pho92 impacts meiotic recombination by controlling key methylated transcripts. bioRxiv, 2022.2003.2021.485107. 10.1101/2022.03.21.485107.

Shen, L., Liang, Z., Gu, X., Chen, Y., Teo, Zhi Wei N., Hou, X., Cai, Weiling M., Dedon, Peter C., Liu, L., and Yu, H. (2016). N6-methyladenosine RNA modification regulates shoot stem cell fate in Arabidopsis. Dev. Cell *38*, 186-200. 10.1016/j.devcel.2016.06.008.

Shi, H., Wang, X., Lu, Z., Zhao, B.S., Ma, H., Hsu, P.J., Liu, C., and He, C. (2017). YTHDF3 facilitates translation and decay of N6-methyladenosine-modified RNA. Cell Res. *27*, 315-328. 10.1038/cr.2017.15 https://www.nature.com/articles/cr201715#supplementary-information.

Sievers, F., Wilm, A., Dineen, D., Gibson, T.J., Karplus, K., Li, W., Lopez, R., McWilliam, H., Remmert, M., Söding, J., et al. (2011). Fast, scalable generation of high-quality protein multiple sequence alignments using Clustal Omega. Mol. Syst. Biol. *7*, 539.

Soltis, D.E., Bell, C.D., Kim, S., and Soltis, P.S. (2008). Origin and Early Evolution of Angiosperms. Ann. N. Y. Acad. Sci. *1133*, 3-25. https://doi.org/10.1196/annals.1438.005.

Sommer, S., Lavi, U., and Darnell, J.E. (1978). The absolute frequency of labeled N-6-methyladenosine in HeLa cell messenger RNA decreases with label time. Journal of Molecular Biology *124*, 487-499. https://doi.org/10.1016/0022-2836(78)90183-3.

Theler, D., Dominguez, C., Blatter, M., Boudet, J., and Allain, F.H. (2014). Solution structure of the YTH domain in complex with N6-methyladenosine RNA: a reader of methylated RNA. Nucleic Acids Res. *42*, 13911-13919. 10.1093/nar/gku1116.

Wang, L., and Roossinck, M.J. (2006). Comparative analysis of expressed sequences reveals a conserved pattern of optimal codon usage in plants. Plant Mol. Biol. *61*, 699-710. 10.1007/s11103-006-0041-8.

Wang, X., Lu, Z., Gomez, A., Hon, G.C., Yue, Y., Han, D., Fu, Y., Parisien, M., Dai, Q., Jia, G., et al. (2014a). N6-methyladenosine-dependent regulation of messenger RNA stability. Nature *505*, 117-120. 10.1038/nature12730.

Wang, X., Zhao, Boxuan S., Roundtree, Ian A., Lu, Z., Han, D., Ma, H., Weng, X., Chen, K., Shi, H., and He, C. (2015). N6-methyladenosine modulates messenger RNA translation efficiency. Cell *161*, 1388-1399. https://doi.org/10.1016/j.cell.2015.05.014.

Wang, Y., Li, Y., Toth, J.I., Petroski, M.D., Zhang, Z., and Zhao, J.C. (2014b). N6-methyladenosine modification destabilizes developmental regulators in embryonic stem cells. Nature cell biology *16*, 191-198. 10.1038/ncb2902.

Wei, L.-H., Song, P., Wang, Y., Lu, Z., Tang, Q., Yu, Q., Xiao, Y., Zhang, X., Duan, H.-C., and Jia, G. (2018). The m6A Reader ECT2 Controls Trichome Morphology by Affecting mRNA Stability in Arabidopsis. Plant Cell *30*, 968-985. 10.1105/tpc.17.00934.

Weijers, D., Franke-van Dijk, M., Vencken, R.-J., Quint, A., Hooykaas, P., and Offringa, R. (2001). An Arabidopsis Minute-like phenotype caused by a semi-dominant mutation in a RIBOSOMAL PROTEIN S5 gene. Development *128*, 4289-4299. 10.1242/dev.128.21.4289.

Worpenberg, L., Paolantoni, C., Longhi, S., Mulorz, M.M., Lence, T., Wessels, H.-H., Dassi, E., Aiello, G., Sutandy, F.X.R., Scheibe, M., et al. (2021). Ythdf is a N6-methyladenosine reader that modulates Fmr1 target mRNA selection and restricts axonal growth in Drosophila. EMBO J. *40*, e104975. https://doi.org/10.15252/embj.2020104975.

867 Xu, C., Wang, X., Liu, K., Roundtree, I.A., Tempel, W., Li, Y., Lu, Z., He, C., and Min, J. (2014).
868 Structural basis for selective binding of m6A RNA by the YTHDC1 YTH domain. Nat. Chem. Biol. *10*,
869 927-929. 10.1038/nchembio.1654
870 http://www.nature.com/nchembio/journal/v10/n11/abs/nchembio.1654.html#supplementary-
871 information.

872 Zaccara, S., and Jaffrey, S.R. (2020). A Unified Model for the Function of YTHDF Proteins in
873 Regulating m(6)A-Modified mRNA. Cell *181*, 1582-1595.e1518. 10.1016/j.cell.2020.05.012.

874 Zhong, S., Li, H., Bodi, Z., Button, J., Vespa, L., Herzog, M., and Fray, R.G. (2008). MTA is an
875 Arabidopsis messenger RNA adenosine methylase and interacts with a homolog of a sex-specific
876 splicing factor. Plant Cell *20*, 1278-1288. 10.1105/tpc.108.058883.

877 Zhu, T., Roundtree, I.A., Wang, P., Wang, X., Wang, L., Sun, C., Tian, Y., Li, J., He, C., and Xu, Y.
878 (2014). Crystal structure of the YTH domain of YTHDF2 reveals mechanism for recognition of N6-
879 methyladenosine. Cell Res. *24*, 1493-1496. 10.1038/cr.2014.152.

880 Zuckerkandl, E., and Pauling, L. (1965). Evolutionary divergence and convergence in proteins. In
881 Evolving Genes and Proteins, V. Bryson, and H.J. Vogel, eds. (Academic Press), pp. 97-166.
882 citeulike-article-id:3198062.
883

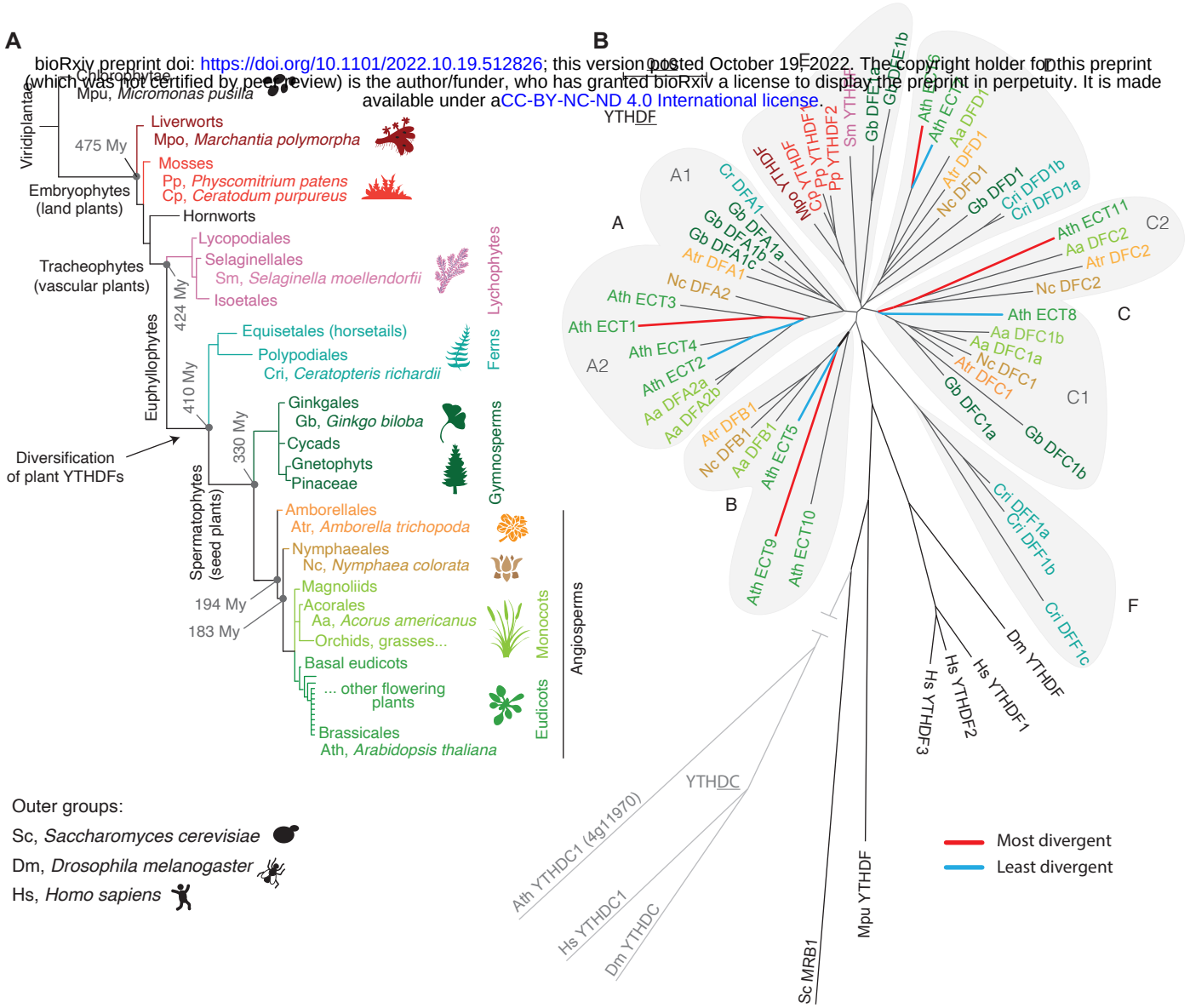

Figure 1. Phylogenetic analysis of YTHDF proteins in land plants

A. Schematic representation of land plant evolution and relative position of the species used in this study. The architecture of the diagram and the age (million years, My) indicated on some nodes are a simplified version of the dated tree from Magallón et al. (2013). The length of the branches has been adjusted for illustrative purposes.

B. Phylogenetic tree of YTHDF proteins in land plants. *Arabidopsis thaliana* (Ath) YTHDF proteins are named after the first nomenclature for proteins containing an Evolutionarily Conserved C-Terminal Region (ECT) established by Ok et al. (2005), while members from other plant species adhere to the nomenclature based on phylogenetic relationships as defined by Scutenaire et al. (2018), with small variations reflecting the additional clades (E, F) and early divergences between subclades (A1 vs A2, and C1 vs. C2) proposed here. Colour-coding and abbreviations of species as in A. Thick red and blue branches highlight, respectively, the most and least divergent ECTs within each clade.

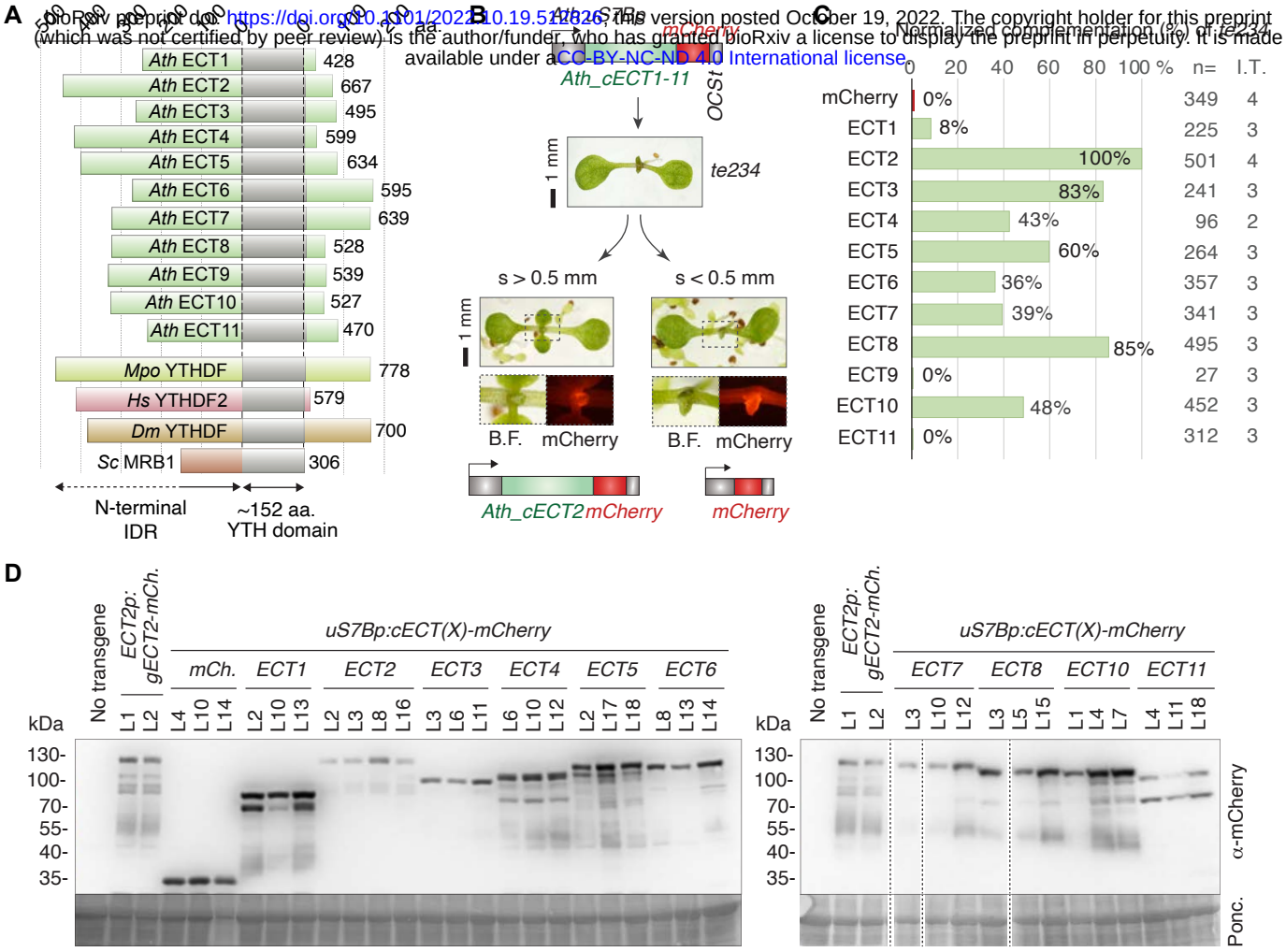

Figure 2. Most Arabidopsis YTHDF proteins can replace ECT2/3/4-function to some extent

A. Diagram showing the relative length of the N-terminal IDRs of *Arabidopsis thaliana* (*Ath*) YTHDF proteins (ECT1-ECT11) together with *Marchantia polymorpha* (*Mpo*) YTHDF, *Homo sapiens* (*Hs*) YTHDF2, *Drosphila melanogaster* (*Dm*) YTHDF, and *Saccharomyces cerevisiae* (*Sc*) MRB1. Numbers on the right side indicate the length of the proteins in amino acids (aa).

B. Schematic representation of the strategy followed for the functional assay. *uS7Bp:cECT(X)-mCherry* constructs are introduced in *ect2-1/ect3-1/ect4-2* (*te234*) plants, and complementation rates are estimated by the percentage of primary transformants (T1) whose first true leaves have a size (s) of at least 0.5 mm after 10 days of growth. The construct *uS7Bp:mCherry* is used as negative control. Examples of T1 seedlings expressing ECT2 and control constructs are shown. Dashed lines delimit the magnified images of emerging leaves with mCherry fluorescence shown below.

C. Weighed averages of the complementation percentages observed for each *uS7Bp:cECT(X)-mCherry* construct in 2-5 independent transformations (I.T.) normalized to the fraction of complementing *uS7Bp:cECT2-mCherry* observed in the same transformation batch. The absolute complementation percentages for each construct in each independent transformation can be found in Figure S3. Examples of complementing T1 plants and the fluorescent signal are shown in Figure S4. n, number of T1s assessed.

D. Levels of protein expression from *uS7Bp:cECT(X)-mCherry* constructs in independent lines (L) of 9-day-old T2 seedlings assesed by α-mCherry western blot. All genotypes are in the *te234* background. Lines with single insertions and the highest complementation capacity (largest true leaves at 9 days after germination in T2) were selected for the analysis. ECT9 is not included because we could not observence fluorescence in the T2 generation for any of the few lines obtained, probably due to silencing. *te234 ECT2p:gECT2-mCherry* lines (Arribas-Hernández et al. 2018) are included in both membranes as a reference. Vertical dotted lines in the right panel mark where lanes have been cropped due to defects in the gel, but all the ones shown are on the same membrane. Ponceau-staining is shown as loading control.

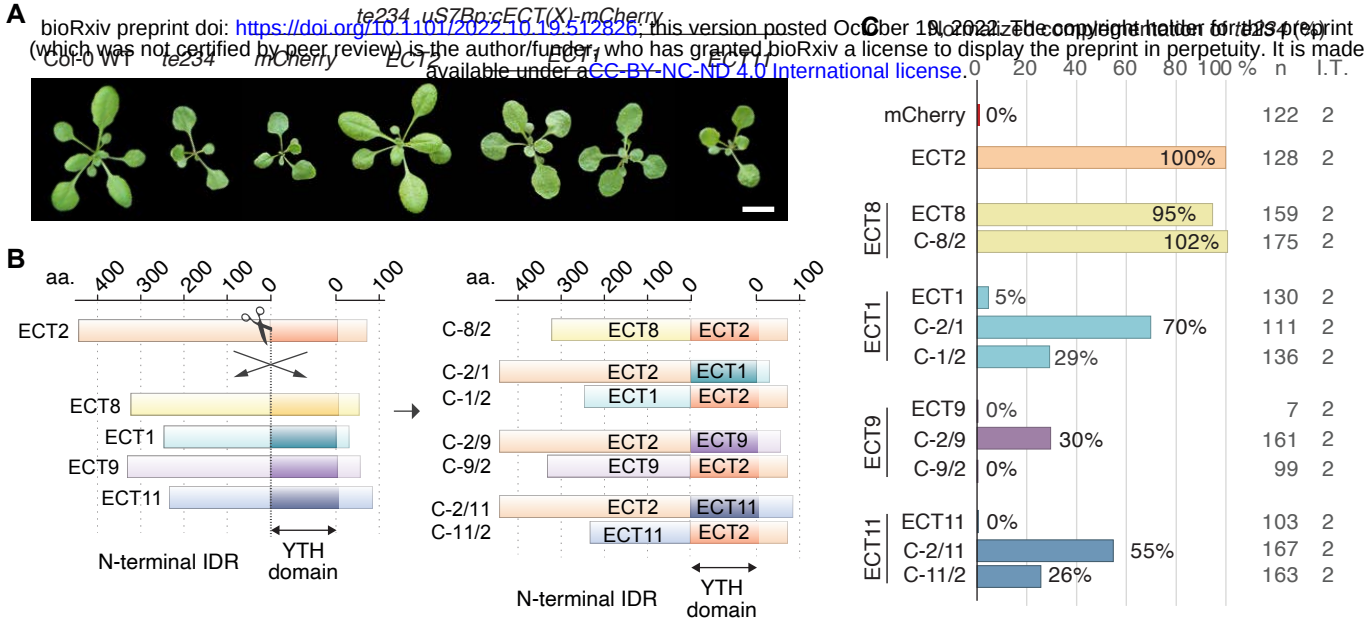

Figure 3. Dissection of ECT1/9/11 functionality by expression of chimeric constructs

A. 20-day-old T2 seedlings expressing the mCherry fusions of ECTs less able to complement the leaf emergence delay of *te234* mutants. For ECT1, the two best complementing lines among 225 T1s were chosen for the phenotypic characterization. Lines expressing ECT11 are indistinguishable from the *te234* background. ECT9 is not included because we could not find lines with fluorescence in T2 seedlings. ECT2, free mCherry, the background *te234* and Col-0 WT are shown as a reference. Scale bars, 1 cm.

B. Schematic representation of the strategy followed to express chimeras with N-terminal IDR and YTH domains of different ECT proteins.

C. Weighed averages of the complementation rates observed for each chimeric construct as in Figure 2C. The absolute complementation rates can be found in Figure S7.

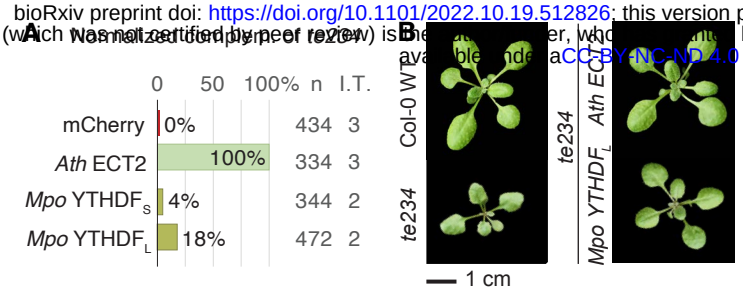

Figure 4. Expression of *Marchantia polymorpha* YTHDF alleviates loss of ECT2/3/4 in *Arabidopsis*

A. Weighed averages of the complementation rates observed for each of the indicated constructs (cDNA fused to mCherry under the control of the *uS7B* promoter) as in Figure 2C. S (short) and L (long) refer to the two different YTHDF splice-forms found among the constructs obtained from *M. polymorpha* cDNA. Absolute complementation rates can be found in Figure S9.

B. T1 plants expressing the long isoform (L) of *uS7Bp:Mpo_cYTHDF-mCherry* in the *te234* background 19 days after germination. Additional genotypes are included as a reference. Pictures of the *Mpo* YTHDF short isoform, other controls and T2 plants can be found in Figure S10.

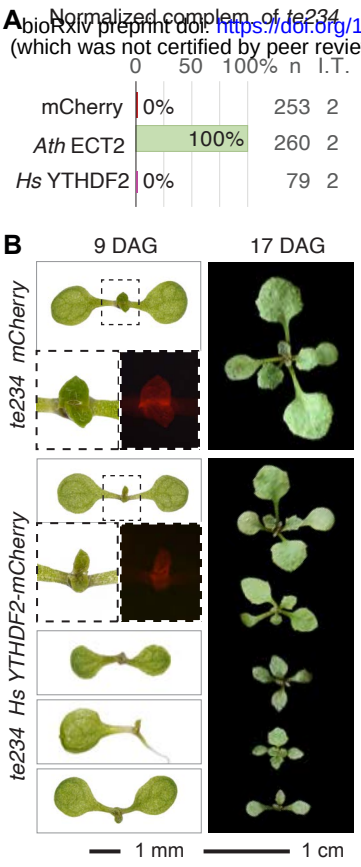

Figure 5. Heterologous expression of *Homo sapiens* YTHDFs enhances the phenotype caused by loss of ECT2/3/4 in *Arabidopsis*

A. Weighted averages of the complementation rates observed for each of the indicated constructs (cDNA fused to mCherry under the control of the *uS7B* promoter) as in Figure 2C. Absolute complementation rates can be found in Figure S9.

B. Morphological appearance and fluorescence pattern of T2 plants expressing *uS7Bp:Hs_cYTHDF2-mCherry* in the *te234* background 9 or 17 days after germination (DAG). Several plants are shown to reflect the variable penetrance of the defects exhibited by these lines compared to the control *te234* expressing free mCherry (top panel). The defects include enhanced aberrance in the shape or number of cotyledons and first true leaves, and slower overall growth. Additional individuals and controls can be found in Figure S10.

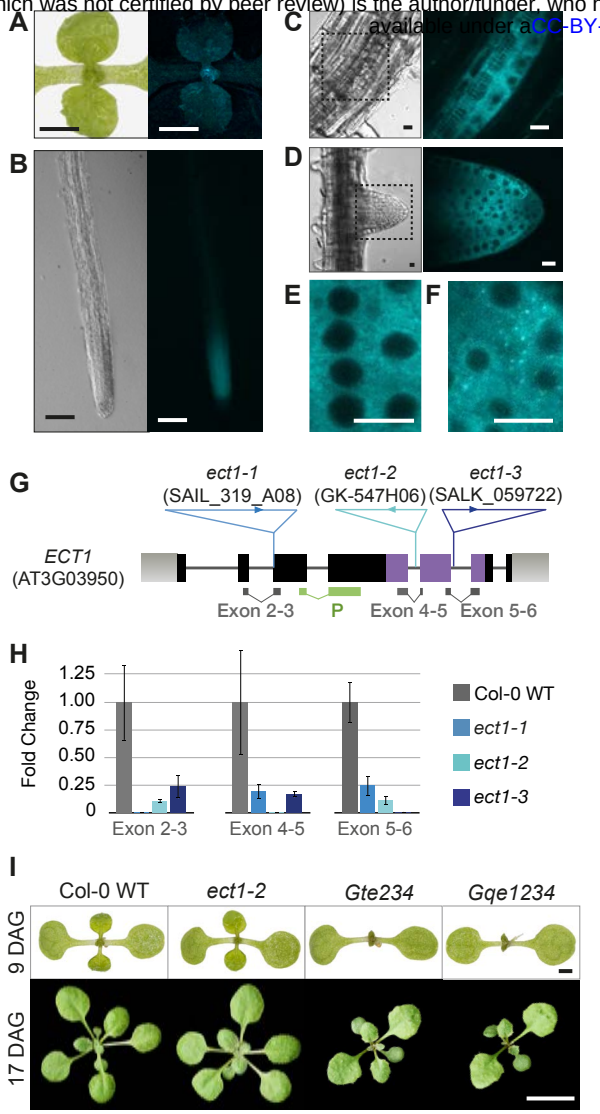

Figure 6. Endogenous ECT1 has negligible ECT2/3/4-like function, despite similar expression pattern and subcellular localization

A-D. Expression pattern of *ECT1p:gECT1-TFP* (gDNA) in aerial organs (B), main root (C), lateral root primordia (D) and emerging lateral roots (E) of 10-day-old seedlings. The expression mimicks the pattern observed for ECT2/3/4 (Arribas Hernández et al., 2020).

E-F. Intracellular localization of ECT1-TFP in meristematic cells of root tips in unchallegended conditions. Although the cytoplasmic signal is largely homogenous (F), sporadic foci (G) are frequently observed. Figure S11A shows the integrity of the fluorescently tagged protein in independent transgenic lines assesed by protein blot.

G. Schematic representation of the *Ath_ECT1* locus. Exons are represented as boxes and introns as lines. The positions and identifiers of the T-DNA insertions assigned to the *ect1-1*, *ect1-2* and *ect1-2* alleles are marked, and the location of qPCR amplicons and hybridization probes (P) for analyses is indicated below.

H. Expression analysis of *ECT1* mRNA in wild type and T-DNA insertion lines by qPCR. Northern blot using the probe (P) marked in G detects *ECT1-TFP* mRNA, but not the endogenous *ECT1* transcript (Figure S11B).

I. Morphological appearance of seedlings with or without *ECT1* in the different backgrounds indicated. Alternative allele combinations are shown in Figure S11D. DAG, days after germination.

Scale bars are: 1 cm in A, 1 mm in B, 100 μm in C, 10 μm in D-F, 1 mm in upper panels of I, and 1 cm in the lower panels.